Anticancer Efficacies of Cisplatin-Releasing pH-Responsive Nanoparticles

Peisheng Xu,[†] Edward A. Van Kirk,[‡] William J. Murdoch,*[,‡] Yihong Zhan,[†] Dale D. Isaak,[§] Maciej Radosz,[†] and Youqing Shen*[,†]

Soft Materials Laboratory and Department of Chemical and Petroleum Engineering, Department of Animal Science and Reproductive Biology Program, and Department of Molecular Biology, University of Wyoming, Laramie, Wyoming 82071

Received November 27, 2005; Revised Manuscript Received January 16, 2006

The objective of these investigations was to test the hypothesis that a rapid cytoplasmic release profile from nanoparticles would potentiate the anticancer activity of cisplatin. Cisplatin-loaded nanoparticles with pH-responsive poly[2-(*N*,*N*-diethylamino)ethyl methacrylate] (PDEA) cores were synthesized from PDEA-*block*-poly(ethylene glycol) (PDEA−PEG) copolymer by using a solvent-displacement (acetone−water) method. Nanoparticles with pH-nonresponsive poly(ϵ-caprolactone) (PCL) cores made from PCL-*block*-PEG (PCL−PEG) were used for comparison. Nanoparticle sizes, ζ potentials, drug-loading capacities, and pH responsiveness were characterized. The cellular uptakes and localization in lysosomes were visualized by using confocal fluorescence microscopy. Cytostatic effects of free and encapsulated *cis*-diammineplatinum(II) dichloride (cisplatin) toward human SKOV-3 epithelial ovarian cancer cells were estimated by using the MTT assay. Intraperitoneal tumor responses to cisplatin and cisplatin/PDEA−PEG were evaluated in athymic mice at 4−6 weeks postinoculation of SKOV-3 cells. PDEA−PEG nanoparticles dissolved at pH < 6 and rapidly internalized and transferred to lysosomes; it therefore was predicted that the PDEA nanoparticles would rapidly release cisplatin into cytoplasm upon integration into acidic lysosomes and thereby overwhelm the chemoresistant properties of SKOV-3 cells. Indeed, relative proportions of viable cells were diminished to a greater extent by exposure in vitro to fast-releasing nanoparticles compared to slow-releasing nanoparticles or an equivalent dose of free cisplatin. Incidences of cellular pyknosis (a morphological indicator of apoptosis) were most evident within intestinal/mesentery tumors of mice treated with cisplatin/PDEA−PEG; tumor burdens were correspondingly reduced.

Introduction

Common (epithelial) ovarian cancer is a deadly insidious disease because it typically remains asymptomatic until it has advanced into the abdominal cavity. Treatment generally entails cytoreductive surgery used in combination with genotoxic platinum-based drugs, most notably *cis*-diammineplatinum(II) dichloride (cisplatin). Notwithstanding, the majority of patients become refractory to chemotherapy and relapse.[1,2] The major cause is the cancer cell's inherent and acquired drug resistance. Alterations in plasma membrane phospholipid dynamics, which restrict drug internalization, and drug detoxification and enhanced DNA repair, which diminish rates of apoptosis, and multidrug resistance, contribute to resistance.[3−6] The activation of P-glycoprotein pumps, the energy-dependent efflux transporters, is a major mechanism of multidrug resistances. P-gp pumps are efficient in binding and exporting drugs as they traverse the plasma membrane.[3,4] Thus, the combination of slow drug entry, efficient removal by the P-gp pumps, and the consumption by other forms of resistance causes the cytoplasmic drug concentration to be diminished below the cell-killing threshold and, thus, a limited therapeutic efficacy. Therefore, to have a high therapeutic efficacy, the available drug in the cell must be more than the drug removal and consumption capacity of the drug resistance.

A variety of carriers,[7] including water soluble polymers,[8,9] dendrimers,[10] liposomes,[11,12] and polymeric micelles (nanoparticles),[13−16] have been shown to efficiently deliver drugs into cells, but carriers that can rapidly release drugs into cytoplasm have a higher therapeutic efficacy. For example, pH or temperature-induced rupturing of liposomes[17−20] or pH-catalyzed hydrolysis of drug−polymer linkages in polymer drugs,[21,22] have rapid drug release rates and, thus, high drug efficacy.

A more prospective approach to fast-cytoplasmic drug release to cancer cells is to use lysosomal pH-triggered fast drug release nanoparticles as drug vehicles. Nanoparticles, because of their stability and submicrometer sizes, are readily internalized via endocytosis and end up in endosomes and lysosomes,[13−16] where the pHs are about 5.5 (endosomes) and 5 (lysosomes).[23,24] Thus, theoretically, rapid cytoplasmic drug release will be achieved if the nanoparticles can dissolve in the acidic endosomes or lysosomes and then rapidly rupture their membranes. Recently, Bae et al. developed pH-sensitive nanoparticles by using poly(L-histidine) or sulfonamide-containing pullulan as the cores.[25−30] The polymers could be protonated at the pH lower than 7, and thus, their nanoparticles dissociated to release the carried drug at pHs less than 7. Such drug-loaded nanoparticles showed higher cytotoxicity at low pH values.[25−30] These nanoparticles, however, may not be efficient for cytoplasmic drug delivery to the cells in solid tumors because their dissolving pH is close to 7, and thus, they destabilize and release drug in the extracellular fluids of solid tumors, where the pH is as low as 6.[31] The drug

* To whom correspondence should be addressed. E-mail: sheny@uwyo.edu (Y.S.) or wmurdoch@uwyo.edu (W.J.M.).

[†] Soft Materials Laboratory and Department of Chemical and Petroleum Engineering.

[‡] Department of Animal Science and Reproductive Biology Program.

[§] Department of Molecular Biology.

10.1021/bm050902y CCC: $33.50
Published on Web 02/15/2006

Scheme 1. Synthesis of PCL−PDMA (A) and PDEA−PEG (B)

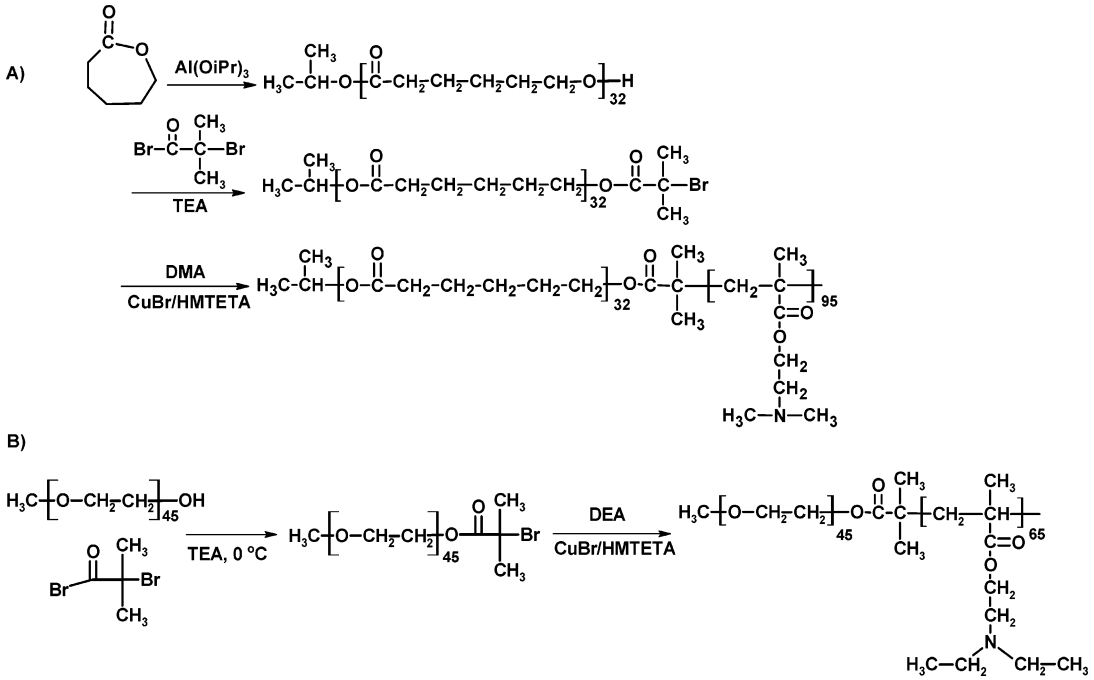

released in the extracellular fluid has difficulty reaching the cytoplasm because of the overexpressed P-gp pumps in the cell membrane.

Herein, we report cisplatin-containing nanoparticles with lysosomal pH-sensitive cores, and we screened their relative cytostatic efficacies against a human ovarian adenocarcinoma cell line. Antitumor activities were assessed in xenografted mice.

Materials and Methods

Reagents were purchased from Sigma-Aldrich (St. Louis, MO) unless indicated otherwise. ϵ-Caprolactone was dried over calcium hydride with stirring for 24 h at room temperature. Tetrahydrofuran (THF) was dried by refluxing over calcium hydride. 2-(*N*,*N*-Dimethylamino)ethyl methacrylate (DMA) and 2-(*N*,*N*-diethylamino)ethyl methacrylate (DEA) were distilled and stored at −20 °C. Purities of 1,1,4,7,10,10-hexamethyltriethylenetetramine (HMTETA), methyl α-bromophenylacetate (MBP), triethylamine, *N*-phenyl-2-naphthylamine (PNA), and 2-bromoisobutyryl bromide were higher than 97%.

Synthesis of Block Copolymers. Poly[2-(*N*,*N*-diethylamino)ethyl methacrylate]-*block*-poly(ethylene glycol) (PDEA−PEG) and poly(ϵ-caprolactone)-*block*-poly[2-(*N*,*N*-dimethylamino)ethyl methacrylate] (PCL−PDMA) block copolymers were synthesized by using atom-transfer radical polymerization (ATRP), as shown in Scheme 1. PCL_{23000}−PEG_{2000} (subscripts denote molecular weights, MW) block copolymer was synthesized as described elsewhere.[32]

Polymer MW and polydispersity were determined by gel permeation chromatography (GPC); the system was equipped with a Waters (Milford, MA) 2414 refractive index detector and two 300-mm solvent-saving GPC columns (MW ranges: 5×10^2−3×10^4, 5×10^3−6×10^5) run at a flow rate of 0.30 mL/min, with THF as solvent at 30 °C. Data were processed by using the Waters software package.

PCL−PDMA synthesis (Scheme 1A). ω-Hydroxy-PCL was synthesized via ring-opening polymerization catalyzed by aluminum isopropoxide;[33] it reacted with 2-bromoisobutyryl bromide to form ω-(2-bromoisobutyrate)-PCL macroinitiator, which initiated the polymerization of DMA with the catalysis of CuBr/HMTETA and produced the PCL−PDMA block copolymer. A typical synthesis was as follows. ϵ-Caprolactone (21.4 mL, 193 mmol), 2-propanol (0.78 mL, 10.1 mmol), and dry THF (22 mL) were injected into a predried flask under nitrogen atmosphere. Aluminum isopropoxide (0.072 g, 0.35 mmol) dissolved in dried THF was added to the reaction system and stirred at 45 °C for 17 h. Polymer was precipitated in 10-fold methanol with 0.1% HCl. PCL was isolated and dried under high vacuum for 24 h (MW 3700, polydispersity 1.3).

The prepared ω-hydroxy-PCL (2.55 g, 0.689 mmol) was dissolved in 50 mL of THF in a three-neck flask. Triethylamine (0.76 mL, 5.42 mmol) was added, and the solution was cooled to 0 °C. 2-Bromoisobutyryl bromide (0.335 mL, 2.71 mmol) was added dropwise, and the mixture was stirred overnight at room temperature. Precipitate was removed by filtration. The solution was concentrated by rotary evaporation, and the polymer was precipitated (×3) in 10-fold excess methanol and dried under vacuum.

CuBr (14 mg, 0.1 mmol) and HMTETA (19.2 μL, 0.07 mmol) were charged to a septum-sealed Schlenk tube. Distilled toluene (0.5 mL) and DMA (0.36 mL, 2.1 mmol) were added and degassed for 5 min. PCL−macroinitiator (0.326 g) in 0.5 mL of degassed toluene was added. The tube was immersed in a 65 °C water bath for 11.5 h. At different time intervals, aliquots were taken by using degassed syringes to monitor the polymerization progress. The polymer was purified by dissolving the mixture in toluene and passing the solution through a silicon gel column to remove the catalyst. The product was precipitated in 10-fold cold hexane (×2) and dried under high vacuum before use (MW PCL_{3700}−$PDMA_{15000}$).

PDEA−PEG synthesis (Scheme 1B). PDEA−PEG was synthesized by a two-step method. PEG−macroinitiator was prepared by reaction of 2-bromoisobutyryl bromide with PEG_{2000}. CuBr (11.9 mg, 0.082 mmol) and HMTETA (22.6 μL, 0.083 mmol) were charged to a Schlenk tube. Distilled toluene (0.5 mL) was added, and the solution was degassed for 5 min with stirring. Distilled DEA (1 mL) was added and degassed for an additional 5 min. Macroinitiator PEG−Br (0.178 g, 0.089 mmol) in degassed toluene was added. The tube was immersed in a 60 °C water bath for 80 min. The reaction was terminated by cooling to room temperature. The solution was diluted with toluene and passed through a column of silica gel to remove the catalyst. Polymer was precipitated in 10-fold cold hexane and dried under high vacuum for 24 h. The MW of the polymer was $PDEA_{12000}$−PEG_{2000}.

Preparation of Cisplatin-Loaded Nanoparticles. Nanoparticles were prepared by acetone displacement. With stirring, copolymer (2.5 mg) was dissolved in 2.5 mL of acetone, and cisplatin (1.0 mmol/L in acetone, 166 μL) was added. The resultant solution was added dropwise

into 5 mL of RPMI-1640 media and stirred overnight to form micelles. Acetone was removed under reduced pressure for 8 h.

Nanoparticles for in vivo treatments were prepared as described above by using 35 mg of copolymer dissolved in 2 mL of acetone, with 6.6 mg of cisplatin in 0.66 mL of acetone added into 1 mL of phosphate-buffer saline (PBS). Loading efficacy was deduced by measuring nonentrapped cisplatin in the centrifugal filtrate. About 0.2 mL of filtrate was filtered from the nanoparticle solution (1.5 mL) by using Centricon YM-3 (Millipore, Billerica, MA, USA; 7000 g, 45 min; $n = 5$), and the cisplatin concentration was determined by inductively coupled plasma mass spectrometry (ELAN 6000; Perkin-Elmer, Wellesley, MA).

Nanoparticle Sizes and ζ Potentials. Sizes and ζ potentials of the nanoparticles were measured with a Zetasizer Nano-ZS (Malvern Instruments, Southborough, MA). Suspensions were sonicated for 30 s. Measurements were performed in disposable sizing cuvettes, using 632.8-nm laser light set at a scattering angle of 173°. Each measurement was performed in triplicate, and the results were processed with Dispersion Technology Software version 3.32.

Polymer Solubility Transition pH. The pH above which the polymer becomes insoluble (transition pH, pH_c) was estimated by fluorescence spectroscopy (SpectraMax Gemini XS; Molecular Devices, Sunnyvale, CA) by using *N*-phenyl-2-naphthylamine (PNA) as a probe (excitation wavelength = 340 nm, emission intensity = 418 nm). PNA has a high fluorescence activity in a hydrophobic environment and low activity in an aqueous medium.[32] Used concentrations of polymers in pH_c measurements were higher than critical micelle concentrations determined as reported previously.[32]

PNA−acetone solution (200 μL, 1.0×10^{-3} mol/L) was added to a brown bottle; the acetone was evaporated, leaving 2.0×10^{-7} mol of PNA. PDEA−PDMA (70 mg) dissolved in HCl-acidified deionized water (pH 4.5) was added, and the solution was adjusted to pH 7.4 with NaOH (0.01 N). The mixture was stirred at 60 °C for 3 h and sonicated for 30 s. HCl (0.01 and 0.1 N) was used to decrease the pH to 4. Fluorescent intensities of solutions at different pH values (3.2−7.4) were assessed.

Lysosome Localization of PDEA−PEG Nanoparticles Observed with Confocal Fluorescent Scanning Microscopy. SKOV-3 cells were obtained from American Type Culture Collection (ATCC, Rockville, MD) and were plated onto glass-bottom petri dishes (MatTek, Ashland, MA, no. P35G-1.0-14-C) at 80 000 cells per plate in 2 mL of media (RPMI-1640, Sigma-Aldrich, supplemented with 10% FBS). They were incubated for 18 h at 37 °C and 5% CO_2 before treatment. Treatments were prepared in media containing 10 mM HEPES, pH 7.4. Lysotracker (Molecular Probes, Carlsbad, CA) was used at 150 nM. Nanoparticles loaded with PHK26 (Aldrich) were prepared similarly. Briefly, PDEA−PEG (2.25 mg) was dissolved in 0.9 mL of methanol with 2.25×10^{-8} mol PHK26 dye. The solution was dropwise added to RPMI medium (4.5 mL) and stirred for several hours. Methanol in the solution was completely removed by using vacuum, and then DI water was added to bring back the solution volume to 4.5 mL. This solution was diluted by 40 times in HEPES-containing RPMI medium for experiment use. Each well was added with the nanoparticle solution. After 90 min, Lysotracker was added to the wells at a concentration of 150 nM. The images were obtained about 60 min later by using a confocal laser scanning microscope (Leica TCS SP2 microscope). Lysotracker was observed by using a 488-nm laser, and the emission wavelength was read from 510 to 540 nm and expressed as green. Nanoparticles loaded with PHK26 were observed by using a 543-nm laser, and the emission wavelength was read from 550 to 620 nm and expressed as red. Images were produced by using the lasers sequentially with a 63× objective lens. Cells were kept at 37 °C and 5% CO_2 except when being observed on the microscope.

To test for accumulation of free dye in the cells from the nanoparticle solution, 1.6 mL of the nanoparticle solution was filtered through a Centricon filter with a 3000 molecular weight cutoff (Amicon, Bedford, MA, no. YM-3) at 2600 g for 1 h. Free dye (if any) should pass through the filter (filtrate), while nanoparticles would be retained on the filter. The filtrate was then applied to the cells just as the nanoparticle solution was used.

Cytostatic Effects of Cisplatin/Nanoparticles on Epithelial Ovarian Cancer Cells In Vitro. SKOV-3 cells were propagated to confluence in T-75 flasks (Corning Costar, Cambridge, MA) at 37 °C in a humidified atmosphere of 95% air and 5% CO_2 in 15 mL of RPMI-1640 media supplemented with 10% fetal bovine serum, 10 μg/mL insulin, and antibiotic/antimycotic solution (A9909). Cells were harvested from exponential phase cultures with 0.25% trypsin/0.03% EDTA, transferred into culture plates (7.5×10^4 cells/mL, 200 μL/well), and incubated for 47 h. Treatments were added in fresh replacement media (100 μL of cisplatin/nanoparticles solution, $n = 3$; cisplatin = 0.25 μg/mL) for 2 h. MTT (3-[4,5-dimethylthiazol-2-yl]-2,5-diphenyltetrazolium bromide, 10 μL) and detergent (100 μL) reagents (ATCC) were added, and cells were incubated for 2 h, respectively. Absorbances at 570 nm (SpectraMax 190) were recorded.

Antitumor Effects of Cisplatin/Nanoparticles in Immunocompromised Mice. The following experiments were conducted with the approval of the University of Wyoming Animal Care and Use Committee.

Athymic (nu/nu, 6−8 weeks old) mice (BALB/c strain) were inoculated by intraperitoneal (ip) injection with SKOV-3 cells (1×10^7) suspended in 0.1 mL of PBS. Animals were maintained in a pathogen-free environment under controlled temperature (24 °C) and lighting (12L:12D) conditions. Sterilized rodent chow and water were supplied ad libitum.

(A) Acute Effects of the Treatments. At four weeks postinoculation, four groups (four/group) of mice were treated ip with 0.1 mL of PBS (vehicle control), PDEA−PEG (blank nanoparticle control), cisplatin, or cisplatin/PDEA−PEG. Equivalent doses of 10 mg/kg cisplatin were administered. The mice were terminated (cervical dislocation) at 6 h posttreatment to evaluate the acute effects of the treatment. Intestines/mesentery were excised and fixed by immersion in Histochoice (Amersco, Solon, OH). Tumor samples were washed in PBS, dehydrated, cleared, infiltrated with paraffin wax, and cross-sectioned at a thickness of 7 μm. Sections were floated onto microscope slides, air-dried, deparaffinized in xylene, rehydrated, stained in hematoxylin and eosin, and examined by light microscopy. One field from each of three tumors per mouse was subjected to morphometric analyses. Numbers of pyknotic (apoptotic) and healthy cells were counted at 1000× magnification. Vascular spaces were ascertained at 200× with the aid of Optimas image analysis software (Bothell, WA).

(B) Tumor Growth Inhibition. At four weeks postinoculation, an additional four groups of mice were treated twice with PBS, cisplatin, cisplatin/PDEA−PEG, or cisplatin/PCL−PEG ($n = 4$) at 4 and 5 weeks postinoculation and killed at 6 weeks to evaluate the long-term effects of the treatments. Tumor nodules were counted along a 1-cm^2 segment of intestine/mesentery at each of three different sites per animal.

Statistics. Assignments to treatments and selections of fields of microscopic inspection were made at random. Within-animal/subsample data were averaged. Mean comparisons were made by analysis of variance and protected least significant difference or Student *t*-test. Contrasts were considered significant at $P < 0.05$. Data are plotted as means ± standard errors (SE).

Results and Discussion

Polymer and Nanoparticle Syntheses and Characterizations. Our intention was to construct amphiphilic copolymers containing acid-sensitive blocks that, when internalized and exposed to a lysosomal milieu (pH ~ 5), would release their drug reservoir in a burst and kill (cancer) cells by exceeding their resistance mechanisms. Tertiary amine polymers are protonated in an acidic pH.[34] Poly(*N*,*N*-dialkylaminoethyl methacrylate)s are especially attractive candidates as drug carriers because they can be prepared by living radical polymerization[35]

Table 1. Sizes and ζ Potentials of the Nanoparticles

nanoparticle	particle average size (nm)	PDI	ζ potential (mV)
PDEA−PEG	81.9 ± 19.8	0.148	9.09 ± 4.84
PCL−PEG	79.75 ± 9.7	0.187	−14.6 ± 5.40
PCL−PDMA	121.7 ± 25.6	0.120	20.86 ± 10.94

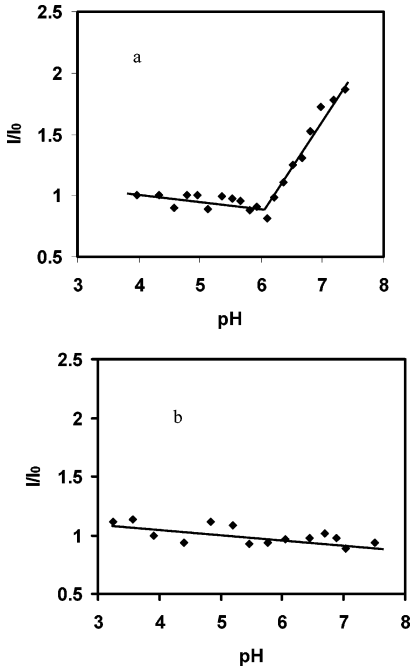

Figure 1. Fluorescence intensity as a function of the solution pH of PNA-loaded PDEA−PEG (a) and PCL−PEG micelles (b) (relative to the fluorescence intensity at pH 4).

and exhibit a low toxicity.[36,37] PDMA is soluble across a wide pH range,[36,37] while PDEA is insoluble at a neutral pH, but is soluble at an acidic pH.[34] PEG or PCL chains with terminal hydroxyl groups were reacted with 2-bromoisobutyryl bromide to introduce ATRP initiator moieties and produce the block copolymers.

Biophysical attributes of the nanoparticles are summarized in Table 1. Sizes ranged from approximately 80 (PDEA/PCL−PEG) to 120 (PCL−PDMA) nm, which is considered ideal for cytoplasmic drug delivery.[38] Nanoparticles with PDMA shells exhibited positive ζ potentials; this is because the tertiary amines of PDMA can be protonated and, thus, carry cationic charges in aqueous solution.[36,37] Micelles of PDEA−PEG had slightly positive ζ potential, suggesting that some of the tertiary amines on the PDEA core surface were protonated. PCL−PEG micelles had a negative ζ potential, consistent with the results in a previous report.[39]

The pH sensitivity of the nanoparticles was evaluated by using a fluorescent PNA probe. PNA has strong fluorescence in a hydrophobic environment, but weak fluorescence in water. Figure 1a shows that the activity of PNA loaded in PDEA−PEG nanoparticles decreased with decreasing pH and reached a minimum at pH of about 6. Correspondingly, the nanoparticles were not detected by dynamic light scattering; these indicate that PDEA cores dissolved at a pH lower than 6 (Figure 1a). In contrast, fluorescence intensities of PNA in nanoparticles with PCL cores were not pH-dependent (Figure 1b), indicative of stability.

Drug-loading efficiencies, calculated as a function of untrapped cisplatin in solution, were 90.1, 73.9, and 97.8% for PCL−PDMA, PCL−PEG, and PDEA−PEG nanoparticles, respectively. Correspondingly, their drug-loading contents were 1.8, 1.48, and 1.96 wt %. The high loading efficiencies were attributed to the high chloride ion concentration in RPMI-1640 and PBS. Cisplatin has a low water solubility. The soluble part of cisplatin can dissociate and release chlorides in water. The dissociation is inhibited by the presence of chloride ions.[40] For example, in 5.8 g/L NaCl solution, only 2% of cisplatin

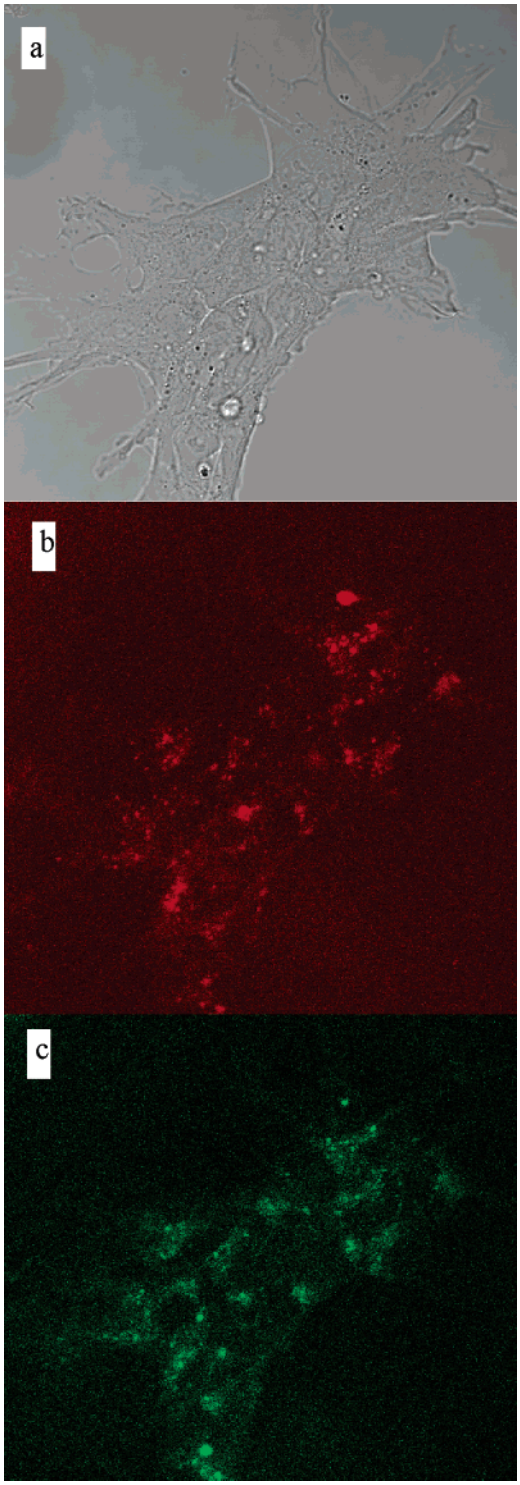

Figure 2. Differential interference contrast (a) and confocal fluorescence scanning microscopy of the cells observed from the red channel (wavelength 550−620 nm) (b), and green channel (510−540 nm) (c). Cells were cultured with PDEA−PEG nanoparticles for 90 min and then lysotracker.

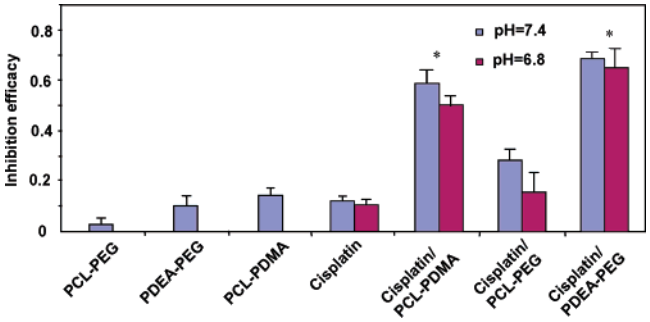

Figure 3. Cytotoxicity of free and nanoparticle-encapsulated cisplatin to SKOV-3 adenocarcinoma cancer cells (2 h treatment) estimated with MTT cell proliferation assay. Cisplatin dose, 0.25 μg/mL. Data represent mean value ± SE ($n = 3$, $P < 0.05$).

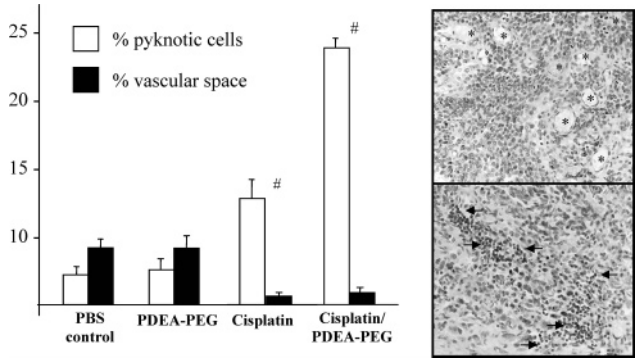

Figure 4. Acute morphological responses of ip ovarian tumors to PDEA−PEG, cisplatin, and cisplatin/PDEA−PEG (6 h after the injection). Representative histological sections are shown of tumor tissues from a vehicle control (upper panel; asterisks are placed in lumens of blood vessels) and a cisplatin/PDEA−PEG-treated (lower panel; arrows indicate pyknotic/condensed cells) animal. Data represent mean value ± SE ($n = 4$, $P < 0.05$).

hydrolyzed in 30 h at 37 °C.[40] Thus, chloride ions decrease the water solubility of cisplatin and force it to be integrated into the hydrophobic PCL and PDEA cores.

Cellular Internalization and Lysosome-Localization of PDEA−PEG Nanoparticles. PDEA−PEG nanoparticles must be internalized and imparted in acidic lysosomes to trigger the fast release of a drug. Thus, the cellular uptake and localization of the nanoparticles were visualized by using confocal fluorescent scanning microscopy. The lysosomes were marked with a lysotracker, while the PDEA−PEG nanoparticles were loaded with PHK26 red fluorescent dye. After being cultured with cells for 150 min, a significant amount of red fluorescent dots were present inside cells. Figure 2b shows a typical image. The cells cultured with filtrate of the nanoparticles (see Materials and Methods) showed no red fluorescence at all. These results indicate that the red fluorescence inside the cell was from the PHK26 dye in the nanoparticles rather than from free dye. This also indicates that a significant amount of nanoparticles were internalized after 150 min of culture.

Comparison of the image of the same cell observed from the lysotracker (green) channel and PHK (red) channel shows that the nanoparticles were localized in the lysosomes. Analysis of others cells (images not shown) confirmed the conclusion. This observation indicates that the PDEA−PEG nanoparticles were indeed trafficked to lysosomes after being internalized.

In Vitro Cytotoxicity to SKOV-3 Cells. Effects in vitro of cisplatin/nanoparticles on SKOV-3 cells are presented in Figure 3. A limitation of the MTT assay is that it does not differentiate net proliferative from death responses. However, in all likelihood, the major cause of cellular losses (during a brief (2 h) incubation) is one of cytotoxicity (doubling times of SKOV-3 cells are ~24 h). PCL−PEG was essentially nontoxic. PDEA−PEG nanoparticles with low positive ζ potentials had some toxicity. The highly positive charged PCL−PDMA had a toxicity similar to free cisplatin.

In general, cisplatin encapsulated in nanoparticles had higher cytotoxicity than the free drug. The inhibitory effect of cisplatin in fast-release PDEA−PEG nanoparticles was significantly greater than that of cisplatin in slow-release PCL−PEG nanoparticles: at a cisplatin dose of 0.25 μg/mL, the inhibition efficiency was 69% for cisplatin/PDEA−PEG, but only 28% for cisplatin/PCL−PEG. To test whether the slight positive charges of the PDEA−PEG nanoparticles (ζ potential +9.09 mv) caused the higher cytotoxicity, slow release PCL−PDMA nanoparticles, which had a significantly higher positive ζ potential (+20.86 mv) than that of PDEA−PEG nanoparticles (Table 1), were compared with PDEA−PEG nanoparticles. Figure 3 shows that cisplatin in the highly positive-charged PCL−PDMA nanoparticles had an inhibition efficiency of about 58%, still lower than cisplatin/PDEA−PEG nanoparticles. These comparisons indicate that the cisplatin in the fast release nanoparticles indeed has higher cytotoxicity than that in slow-releasing nanoparticles.

Different from the poly(L-histidine)-based nanoparticles, which showed higher cytotoxicity at lower pH (6.8) due to the destabilization at this pH,[25] the drug in PDEA−PEG nanoparticles had slightly lower cytotoxicity at pH 6.8 (Figure 3); this is because PDEA−PEG nanoparticles were still stable at this pH and released little of the drug, while the cells were under stress at this low pH and only slowly took up the nanoparticles.

In Vivo Antitumor Activity. The in vivo antitumor activity of cisplatin encapsulated in fast-release nanoparticles was tested by using nude mice xenografted with intraperitoneal ovarian tumors, simulating the advanced metastasis state of the disease in women. The morphometric analyses of histological sections of the mesentery/intestine tumors of the mice were conducted to infer the acute effects of the treatments. Representative photomicrographs are shown of the vehicle control (upper panel; asterisks denote blood vessels) and the cisplatin/PDEA−PEG nanoparticle (lower panel; arrows indicate pyknotic cells in specimens) (Figure 4).

The tumors in the mice injected with PDEA−PEG nanoparticles were not different from those of mice in the control group injected with PBS. They had abundant blood vessels (* shown in the upper panel) and very few pyknotic cells, which display highly condensed pyknotic nuclei, the most characteristic feature of apoptosis, and are considered as dead cells. Therefore, PDEA−PEG nanoparticles alone had no in vivo anticancer activity even though they had some in vitro cytotoxicity to the cells. The tumors treated with cisplatin or cisplatin/PDEA−PEG had significantly more pyknotic cells and less blood vessels. On average, there were 1.5 blood vessels in the examined area in the tumors treated with cisplatin or cisplatin/PDEA−PEG, compared to about 8−9 blood vessels in the tumors of the control group. This is consistent with the suppressing neovascularization effect of cisplatin.[41] The tumors treated with cisplatin/PDEA−PEG had pyknotic cells about twice that in the free cisplatin-treated tumors. This indicates that cisplatin/PDEA−PEG was more efficient in inducing apoptosis, which is consistent with the in vitro results.

Numbers of ovarian tumors were reduced in mice following two treatments with cisplatin, cisplatin/PDEA−PEG, or cisplatin/PCL−PEG (Figure 5). The most marked response oc-

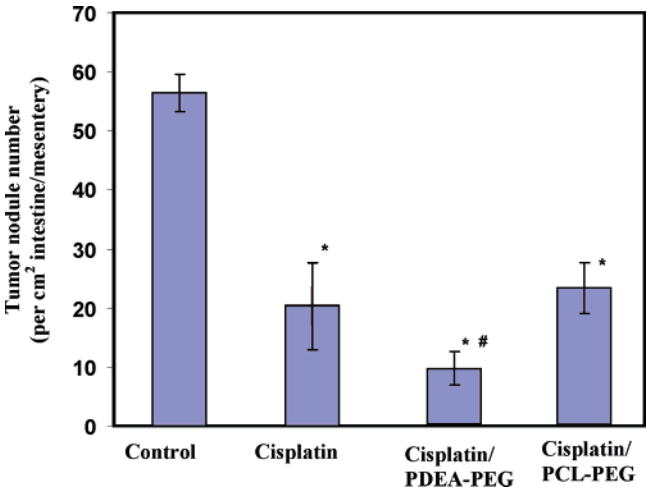

Figure 5. Ovarian tumors in mice treated with vehicle, cisplatin, cisplatin/PDEA−PEG, or cisplatin/PCL−PEG at 4 and 5 weeks after ip inoculation of SKOV-3 cells and killed at 6 weeks. ($n = 4$, * $P < 0.05$ vs control group; # $P < 0.05$ vs free cisplatin and cisplatin/PCL−PEG slow-releasing nanoparticles treatment groups).

curred in the cisplatin/PDEA−PEG group. There was no advantage for cisplatin/PCL−PEG (i.e., a slow-release nanoparticle) compared to cisplatin alone even though cisplatin/PCL−PEG nanoparticles showed in vitro cytotoxicity. The nanoparticles with PDMA outer layers were not tested in vivo because of their possible toxicity to healthy cells.

This is the first report to our knowledge suggesting a potential benefit of fast-releasing cisplatin nanoparticles for ip ovarian cancer therapy. Although we did not observe any overt untoward side effects of the treatments, nonspecific cytotoxicities are a concern. Gonadotropin-releasing hormone and folate receptors, which are overexpressed by epithelial ovarian cancer cells,[42,43] are being exploited for targeting purposes.

Drug release rates from solid nanoparticle cores are typically slow because of attenuated diffusion.[44] Higher cytotoxicities were found in pH-responsive nanoparticles fabricated from poly(L-histidine) and pullulan.[25−30] However, these nanoparticles become soluble at pHs close to 7 and, thus, destabilize and release drugs in the slightly acidic extracellular spaces of solid tumors.[31] Therefore, for cytoplasmic drug delivery by nanoparticles, the transition pH of the nanoparticle must be at pH of about 6 or lower.

PDEA−PEG nanoparticles become soluble at pH of about 6 (Figure 1) and transferred into lysosomes once internalized (Figure 2). We thus propose that, once a PDEA−PEG nanoparticle is localized in a lysosome, it will dissolve immediately through protonation of its amine groups at the acidic pH (<5.5).[23,24] Amine-containing polymers can act as proton sponges, as proposed in the gene delivery.[37] Continuous protonation leads to an influx of electrolytes and, consequently, to osmotic swelling and lysosomal rupture,[37] and finally, the rapid release of the drug into the cytoplasm. Furthermore, a prompt lysosomal escape is important because otherwise the anticancer drug would quickly be degraded and therefore not made available (in high concentrations) for diffusion into the nucleus and DNA binding.

Acknowledgment. This work was supported by grants from the National Science Foundation (BES-0401982) and National Institutes of Health (NIH RR-016474).

Abbreviations

ATRP, atom-transfer radical polymerization
cisplatin, cis-diammineplatinum(II) dichloride
DEA, 2-(*N*,*N*-diethylamino)ethyl methacrylate
DMA, 2-(*N*,*N*-dimethylamino)ethyl methacrylate
GPC, gel permeation chromatography
HMTETA, *N*,*N*,*N*′′,*N*′′′,*N*′′′-hexamethyltriethylenetetramine
ip, intraperitoneal
MBP, methyl α-bromophenylacetate
MW, molecular weight
NMR, nuclear magnetic resonance
PBS, phosphate-buffer saline
PCL, poly(ϵ-caprolactone)
PDEA, poly[2-(*N*,*N*-diethylamino)ethyl methacrylate]
PDI, particle size distribution index
PDMA, poly[2-(*N*,*N*-dimethylamino)ethyl methacrylate]
PEG, poly(ethylene glycol)
pH_c, polymer solubility transition pH
PNA, *N*-phenyl-2-naphthylamine
THF, tetrahydrofuran

References and Notes

(1) Omura, G. A.; Brady, M. F. *Obstet. Gynecol. (N. Y.)* **1993**, *81*, 641.
(2) Naora, H.; Montell, D. J. *Nat. Rev. Cancer* **2005**, *5*, 355.
(3) Agarwal, R.; Kaye, S. B. *Nat. Rev. Cancer* **2003**, *3*, 502.
(4) Gottesman, M. M. *Annu. Rev. Med.* **2002**, *53*, 615.
(5) Doyle, L. A.; Ross, D. D. *Oncogene* **2003**, *22*, 7340.
(6) Duvvuri, M.; Krise, J. P. *Front. Biosci.* **2005**, *10*, 1499.
(7) Moses, M. A.; Brem, H.; Langer, R. *Cancer Cell* **2003**, *4*, 337.
(8) David, A.; Kopeckova, P.; Minko, T.; Rubinstein, A.; Kopecek, J. *Eur. J. Cancer* **2004**, *40*, 148.
(9) Dharap, S. S.; Qiu, B.; Williams, G. C.; Sinko, P.; Stein, S.; Minko, T. *J. Controlled Release* **2003**, *91*, 61.
(10) Gillies, E. R.; Frechet, J. M. J. *Drug Discovery Today* **2005**, *10*, 35.
(11) Vail, D. M.; Amantea, M. A.; Colbern, G. T.; Martin, F. J.; Hilger, R. A.; Working, P. K. *Semin. Oncol.* **2004**, *31*(6, Suppl. 13), 16.
(12) Torchilin, V. P. *Nat. Rev. Drug Discovery* **2005**, *4*, 145.
(13) Kwon, G. S. *Crit. Rev. Ther. Drug Carrier Syst.* **1998**, *15*, 481.
(14) Yang, L.; Alexandridis, P. *Curr. Opin. Colloid Interface Sci.* **2000**, *5*, 132.
(15) Brannon-Peppas, L.; Blanchette, J. O. *Adv. Drug Delivery Rev.* **2004**, *56*, 1649.
(16) Panyam, J.; Labhasetwar, V. *Adv. Drug Delivery Rev.* **2003**, *55*, 329.
(17) Maeda, M.; Kumano, A.; Tirrell, D. A. *J. Am. Chem. Soc.* **1988**, *110*, 7459.
(18) Chen, Q.; Tong, S.; Dewhirst, M. W.; Yuan, F. *Mol. Cancer Ther.* **2004**, *3*, 1311.
(19) Lindner, L. H.; Eichhorn, M. E.; Eibl, H.; Teichert, N.; Schmitt-Sody, M.; Issels, R. D.; Dellian, M. *Clin. Cancer Res.* **2004**, *10*, 2168.
(20) Needham, D.; Anyarambhatla, G.; Kong, G.; Dewhirst, M. W. *Cancer Res.* **2000**, *60*, 1197.
(21) Gillies, E. R.; Frechet, J. M. J. *Bioconjugate Chem.* **2005**, *16*, 361.
(22) Kamada, H.; Tsutsumi, Y.; Yoshioka, Y.; Yamamoto, Y.; Kodaira, H.; Tsunoda, S.; Okamoto, T.; Mukai, Y.; Shibata, H.; Nakagawa, S.; Mayumi, T. *Clin. Cancer Res.* **2004**, *10*, 2545.
(23) Schmid, S.; Fuchs, R.; Kielian, M.; Helenius, A.; Mellman, I. *J. Cell Biol.* **1989**, *108*, 1291.
(24) Barret, A.; Heath, M. In *Lysosomes: A Laboratory Handbook*, 2nd ed.; Dingle, J., Ed.; North-Holland: New York, 1977.
(25) Lee, E. S.; Na, K.; Bae, Y. H. *J. Controlled Release* **2005**, *103*, 405.
(26) Lee, E. S.; Na, K.; Bae, Y. H. *J. Controlled Release* **2003**, *90*, 103.
(27) Lee, E. S.; Shin, H. J.; Na, K.; Bae, Y. H. *J. Controlled Release* **2003**, *90*, 363.
(28) Na, K.; Lee, K. H.; Bae, Y. H. *J. Controlled Release* **2004**, *97*, 513.
(29) Na, K.; Bae, Y. H. *Pharm. Res.* **2002**, *19*, 681.
(30) Kang, S. I.; Na, K.; Bae, Y. H. *Macromol. Symp.* **2001**, *172*, 149.
(31) Helmlinger, G.; Yuan, F.; Dellian, M.; Jain, R. K. *Nat. Med.* **1997**, *3*, 177; Jain, R. K. *J. Controlled Release* **2001**, *74*, 7.
(32) Xu, P.; Tang, H.; Li, S.; Ren, J.; Van Kirk, E. A.; Murdoch, W. J.; Radosz, M.; Shen, Y. *Biomacromolecules* **2004**, *5*, 1736.
(33) Dubois, P.; Jerome, R.; Teyssie, P. *Macromolecules* **1991**, *24*, 977.
(34) Liu, S.; Weaver, J. V. M.; Save, M.; Armes, S. P. *Langmuir* **2002**, *18*, 8350.
(35) Shen, Y.; Zhu, S.; Zeng, F.; Pelton, R. *Macromolecules* **2000**, *33*, 5399.

(36) van Steenis, J. H.; van Maarseveen, E. M.; Verbaan, F. J.; Verrijk, R.; Crommelin, D. J. A.; Storm, G.; Hennink, W. E. *J. Controlled Release* **2003**, *87*, 167.
(37) Van de Wetering, P.; Moret, E. E.; Schuurmans-Nieuwenbroek, N. M. E.; van Steenbergen, M. J.; Hennink, W. E. *Bioconjugate Chem.* **1999**, *10*, 589.
(38) Yokoyama, M. *Drug Delivery Syst.* **1999**, *14*, 449.
(39) Ameller, T.; Marsaud, V.; Legrand, P.; Gref, R.; Barratt, G.; Renoir, J.-M. *Pharm. Res.* **2003**, *20*, 1063.
(40) Wenclawiak, B. W.; Wollmann, M. *J. Chromatgr., A* **1996**, *724*, 317.
(41) Yoshikawa, A.; Saura, R.; Matsubara, T.; Mizuno, K. *Kobe J. Med. Sci.* **1997**, *43*, 109.
(42) Lu, Y.; Low, P. S. *Adv. Drug Delivery Rev.* **2002**, *54*, 675.
(43) Volker, P.; Grundker, C.; Schmidt, O.; Schulz, K. D.; Emons, G. *Am. J. Obstet. Gynecol.* **2002**, *186*, 171.
(44) Fonseca, C.; Simoes, S.; Gaspar, R. *J. Controlled Release* **2002**, *83*, 273.

BM050902Y